Published in final edited form as:
J Immunol. 2012 September 15; 189(6): 2909–2917. doi:10.4049/jimmunol.1103231.

CD28 Promotes CD4+ T Cell Clonal Expansion During infection Independently of its YMNM and PYAP Motifs

Antonio J. Pagán[*], **Marion Pepper**[*,‡], **H. Hamlet Chu**[*,§], **Jonathan M. Green**[†], and **Marc K. Jenkins**[*]

[*]Department of Microbiology and Center for Immunology, University of Minnesota Medical School, Minneapolis, MN, USA 55455

[†]Department of Internal Medicine and Department of Pathology and Immunology, Washington University, St. Louis, MO, USA 63110

Abstract

CD28 is required for maximal proliferation of $CD4^+$ T cells stimulated through their TCRs. Two sites within the cytoplasmic tail of CD28, a YMNM sequence that recruits PI3K and activates NFκB, and a PYAP sequence that recruits Lck, are candidates as transducers of the signals responsible for these biological effects. We tested this proposition by tracking polyclonal peptide:MHCII-specific $CD4^+$ T cells *in vivo* in mice with mutations in these sites. Mice lacking CD28 or its cytoplasmic tail had the same number of naive T cells specific for a peptide:MHCII ligand as wild-type mice. However, the mutant cells produced one-tenth as many effector and memory cells as wild-type T cells following infection with bacteria expressing the antigenic peptide. Remarkably, T cells with a mutated PI3K binding site, a mutated PYAP site, or both mutations proliferated to the same extent as wild-type T cells. The only observed defect was that T cells with a mutated PYAP or Y170F site proliferated even more weakly in response to peptide without adjuvant than wild-type T cells. These results show that CD28 enhances T cell proliferation during bacterial infection by signals emanating from undiscovered sites in the cytoplasmic tail.

Introduction

The generation of a primary $CD4^+$ T cell response to an infection depends on the display of MHCII-bound pathogen-derived peptides (p:MHCII) on the surface of APCs (1). Naïve $CD4^+$ T cells that express TCRs specific for these p:MHCII undergo multiple rounds of division and differentiate into effector cells capable of secreting cytokines that promote the microbicidal activity of other cells (2). Some of these effector T cells then survive the contraction phase to become long-lived quiescent memory cells capable of protecting the host from a second infection (3).

Although necessary, TCR signaling is not sufficient for maximal clonal expansion; concomitant CD28 signaling in response to its APC-displayed ligands CD80 and CD86 is also required. The importance of CD28 is evidenced by the failure of CD28-deficient mice to produce germinal centers and T cell-dependent antibody responses and to clear certain infections (4, 5). At the cellular level, it has been proposed that CD28 acts by enhancing cell

To whom correspondence should be addressed: Marc K. Jenkins, jenki002@umn.edu, Department of Microbiology, Center for Immunology, University of Minnesota Medical School, Minneapolis, MN, USA 55455, Phone: 612-262-2715, Fax: 612-625-2199.
[‡]Present address: University of Washington, Seattle, WA, USA 98195
[§]Present address: University of California, Berkeley, CA, USA 94720

The authors have no conflicting financial interests.

division by augmenting IL-2 mRNA production or stability (6, 7), while other reports indicate that CD28 has no effect on proliferation but promotes cell survival by increasing glucose metabolism (8) or inducing Bcl-x_L (9, 10).

CD28 signal transduction is also unclear. Some studies indicate that the biological effects of CD28 depend on a signal cascade emanating from the YMNM site in the CD28 cytoplasmic tail. Phosphatidylinositol 3-kinase (PI3K) has been reported to bind to the YMNM phosphotyrosine (11), resulting in the recruitment of 3-phosphoinositide-dependent protein kinase (PDK1), Akt, and protein kinase C theta (PKCθ) to the immunological synapse (12, 13). PDK1 and Akt cooperate with PKCθ to activate the Bcl10/Carma1/Malt1 signalosome and subsequently induce translocation of NFkB to the nucleus and transcription of NFκB target genes encoding IL-2 (12, 14–16) and Bcl-x_L (17–19). These results suggest a model in which CD28 ligation in the presence of TCR signaling activates NFκB through PI3K. Akt also activates mammalian target of rapamycin (mTOR) resulting in increased cell cycle activity and glucose metabolism (20–22). The observation that pharmacological inhibition of PI3K limits T cell proliferation and glucose metabolism *in vitro* (8) is consistent with this scenario. This model is challenged, however, by the determination that genetic disruption of the YMNM motif prevented PI3K binding and phosphorylation of Akt with no effect on IL-2 production or T-cell proliferation (23, 24).

Other reports indicate that CD28 signals through the C-terminal PYAP motif (25). Disruption of this site eliminates PKCθ, Filamin A, and Lck recruitment to the CD28 cytoplasmic tail and prevents CD28-dependent enhancement of the immunological synapse (13, 26–33). These results suggest a model in which CD28 signaling causes cytoskeletal changes that indirectly improve TCR signaling by promoting formation of the immunological synapse. This model is supported by the report that genetic disruption of the PYAP site reduced phosphorylation of PKCθ, IL-2 secretion, and impaired T cell proliferation (24).

It is possible that many of the conflicting reports about CD28 signaling relate to the experimental systems used. Many of the aforementioned studies employed transformed cell lines with aberrant TCR signaling machinery, long-term cultured T cell lines, non-p:MHCII stimuli such as mitogens, agonistic antibodies, or superantigens, and adoptive transfer of large numbers of TCR transgenic T cells, which can alter immune homeostasis (34). We circumvented these limitations by studying the contributions of the YMNM and PYAP sites in CD28 during a physiologically relevant *in vivo* response of polyclonal p:MHCII-specific $CD4^+$ T cells to a bacterial infection. We found that CD28 was required to sustain, but not initiate, naive $CD4^+$ T cell proliferation, and suggest that CD28 achieves this effect by signaling independently of the YMNM and PYAP sites in its cytoplasmic tail.

Materials and Methods

Mice

Six-to-eight week old C57BL/6 (B6), B6.PL-Thy1^a/CyJ (*Thy1.1*) mice, B6.SJL-*Ptprc*^{a} *Pepc*^{b}/BoyJ (*Cd45.1*), B6.129S2-*Cd28*^{tm1Mak}/J (*Cd28*$^{-/-}$) (35), and B6.129S7-*Rag1*^{tm1Mom}/J (*Rag1*$^{-/-}$) (36) mice were purchased from The Jackson Laboratory or the National Cancer Institute. *Cd28*$^{-/-}$, *Cd45.1/.2* heterozygotes, *Thy1.1/.2* heterozygotes, *Cd28*$^{AYAA/AYAA}$ (*AYAA*) (25) and *Cd28*$^{Y170F/Y170F}$ (*Y170F*) (24) mice were bred in-house. Bone marrow from *Cd28*$^{AYAA/AYAA\ Y170F/Y170F}$ (*AYAA/Y170F*) mice was provided by J. Green, bone marrow from *Cd28*$^{-/-}$ *full-length Cd28* trangenic and *tail-less Cd28* transgenic mice (37) was provided by A. Singer. Bone marrow from *Prkcq*$^{-/-}$ (38) and *p50*$^{-/-}$ *crel*$^{-/-}$ (39, 40) mice was provided by A. Beg, and *Card11*$^{-/-}$ (41) by M. Farrar. Mice were housed in specific pathogen-free conditions according to guidelines from the University of Minnesota

and the National Institutes of Health. The Institutional Animal Care and Use Committee of the University of Minnesota approved all animal experiments.

L. monocytogenes infection

Mice were injected intravenously with 10^7 colony forming units of Δ*actA L. monocytogenes* bacteria expressing a recombinant protein containing the 2W peptide (EAWGALANWAVDSA) fused to chicken ovalbumin (42).

p:MHCII tetramer production

Soluble 2W:I-A^b and LLOp:I-A^b molecules were produced and biotinylated in *Drosophila melanogaster* S2 cells and then combined with streptavidin-allophycocyanin or streptavidin-PE (Prozyme) to make tetramers, as previously described (43).

p:MHCII tetramer staining and magnetic enrichment

2W:I-A^b and LLOp: I-A^b staining and magnetic enrichment were performed as previously described (44). Briefly, single cell suspensions of spleen and lymph nodes were stained with 10 nM allophycocyanin- or PE-labeled 2W:I-A^b or LLOp: I-A^b tetramers for 1 hour at room temperature. Samples were then incubated with magnetic anti-fluorochrome microbeads and run through a magnetized LS column (Miltenyi Biotec).

Antibodies and flow cytometry

All antibodies were from eBioscience unless noted. Samples were stained at 4°C with Pacific Blue- or eFluor 450-conjugated anti-B220 (RA3-6B2), anti-CD11b (MI-70), anti-CD11c (N418), and anti-F4/80 (BM8, Invitrogen), Pacific Orange-conjugated anti-CD8α (5H10, Invitrogen), FITC-conjugated anti-CD3ε (145-2C11), peridinin chlorophyll protein-cyanine 5.5-conjugated anti-CD3ε (145-2C11), anti-Vα2 (B20.1) or anti-CD4 (RM4-5), Alexa Fluor-conjugated anti-CD44 (IM7), allophycocyanin-Alexa Fluor 750 or allophycocyanin-eFluor 780-conjugated anti-CD4 (RM4-5) antibodies. Samples were run on an LSRII flow cytometer (Becton-Dickinson) and analyzed with FlowJo software (Tree Star).

DNA staining and detection

Tetramer-enriched samples were stained with antibodies against surface antigens and subsequently fixed and permeabilized with eBioscience Fixation and Permeabilization Buffers. Cells were then stained with 4′,6-diamidino-2-phenylindole, dihydrochloride (DAPI) (1μg/ml, Invitrogen) diluted in eBioscience Permeabilization Buffer for one hour at 4°C. The DAPI signal was visualized in linear mode on an LSRII equipped with a UV laser. The DAPI-A and DAPI-W parameters were used to exclude cell aggregates.

Adoptive transfer

Polyclonal $CD4^+$ T cells from the spleen and lymph nodes of wild-type and *Cd28*$^{-/-}$ mice were isolated with a $CD4^+$ T cell isolation kit (Miltenyi Biotec). These were then labeled with CFSE (5μM; Invitrogen) as previously described (45). Four x 10^7 $CD4^+$ T cells were transferred intravenously into individual *Cd90.1* sex-matched recipients. A day after transfer, some mice were infected with Lm-2W bacteria and 2W:I-A^b-specific T cells from the spleen and lymph nodes were magnetically enriched and detected as described above. PE-conjugated anti-CD90.2 (53-2.1) was used to identify donor-derived cells.

Bone marrow irradiation chimeras

Bone marrow cells were harvested from crushed femurs, tibias, and humeri. T cells were depleted from bone marrow cell suspensions with anti-CD90.2 (30-H12) and low toxicity rabbit complement (Cedarlane Laboratories). To generate 50:50 mixed bone marrow chimeras, equal amounts of bone marrow from each donor strain were combined. Recipient mice were irradiated with 1,000 rads and injected intravenously with $5 – 10 \times 10^6$ bone marrow cells. Chimerism in the blood was assessed 8 weeks after reconstitution by determining the percentages of donor-derived B cells or T cells of each strain. FITC-conjugated anti-CD45.2 (104), peridinin chlorophyll protein-cyanine 5.5-conjugated anti-CD45.1 (A20), PE-cyanine 7-conjugated anti-CD90.1 (HIS51), and allophycocyanin-conjugated anti-CD90.2 (53-2.1) antibodies were used to identify donor-derived cells. Variations in the absolute numbers of 2W:I-A^b-specific T cells due to minor differences in chimerism were corrected with the formula, $c = (r/p) \times 50\%$, where p is the percentage of cells among donor-derived cells obtained experimentally, r is the experimentally-determined absolute number of 2W:I-A^b-specific T cells, and c is the absolute number after the correction (46).

Peptide immunization

For analysis of clonal expansion without adjuvant, mice were immunized intravenously with 50μg of 2W peptide (EAWGALANWAVDSA) (GenScript) diluted in PBS.

RelA translocation assay

OT-II CD90.1$^+$ CD4$^+$ T cells were isolated from spleen and lymph nodes with a CD4$^+$ T cell isolation kit (Myltenyi Biotec) and $0.5–1 \times 10^6$ cells were adoptively transferred into CD90.2$^+$ wild-type recipients. The next day, recipient mice were injected intravenously with 5 μg of *Escherichia coli* LPS (List Biological Laboratories) diluted in PBS and then a day later, some mice were iinjected intravenously with 100 μg of chicken ovalbumin peptide 323–339 (OVAp) (Invitrogen) diluted in PBS. Spleens were harvested 20 min after peptide injection, and single cell suspensions of splenocytes were immediately made in 1.5% paraformaldehyde (Electron Microscopy Sciences). CD90.1$^+$ cells were magnetically enriched as previously described (44). Enriched cells were permeabilized in 0.5% saponin (SIGMA) and stained with biotin-conjugated anti-CD90.1 (HIS51), peridinin chlorophyll protein-cyanine 5.5-conjugated streptavidin, PE-conjugated anti-Vβ5 (MR9-4, Pharmingen), AlexaFluor-488-conjugated anti-RelA (F-6, Santa Cruz Biotechnology), and 7-aminoactinomycin D (7AAD) (5μM, Invitrogen). RelA localization was determined with an ImageStream 300 (Amnis Corp.) scanning flow cytometer as previously described (47).

Statistical analyses

Statistical tests were performed with Microsoft Excel or GraphPad Prism software. P values less than 0.05 were considered statistically significant. Comparisons of absolute cell numbers were done on the $\log_{10}$ of each value (i.e., linearized) to minimize differences in statistical variance of the raw values caused by exponential growth. The two-tailed Student's *t* test was used when comparing two groups, and a one-way analysis of variance (ANOVA) with Bonferroni's post-test was performed when comparing three groups. The one-phase exponential decay was used to calculate the half-life of 2W:I-A^{b+} T cells during the contraction (days 5 – 20) and memory (days 20 – 160) phases. Mean absolute numbers of 2W:I-A^{b+} T cells at each time point within a specified time span were used to determine the best-fit values.

Results

CD28 enhances the expansion of polyclonal CD4$^+$ T cells responding to an *L. monocytogenes*-derived p:MHCII *in vivo*

We used p:MHCII tetramers and a magnetic bead-based enrichment method to detect endogenous p:MHCII-specific CD4$^+$ T cells (43, 44) responding to bacterial infection in mice expressing the I-A^b MHCII molecule. The *L. monocytogenes* strain used for these experiments was attenuated due to lack of the *actA* gene product needed by the bacteria to spread from one host cell to another (48), and was engineered to secrete plasmid-encoded chicken ovalbumin fused to a peptide called 2W (AWGALANWA) under control of the *hly* promoter (Lm-2W) (42). These bacteria also secrete listeriolysin O (LLO) expressed from the endogenous *hly* gene on the bacterial chromosome. The 2W peptide and LLO peptide 190–201(LLOp) bind to I-A^b MHCII molecules and stimulate CD4$^+$ T cells in C57BL/6 mice (49, 50). We produced 2W- and LLOp-containing I-A^b streptavidin-fluorochrome tetramers and used them with anti-fluorochrome-conjugated magnetic beads to enrich specific T cells from the spleen and lymph nodes of naïve and infected mice.

We initially sought to determine whether the pre-immune CD4$^+$ T cell repertoires of wild-type and CD28-deficient mice were similar. Uninfected wild-type and CD28-deficient mice contained about 200 2W:I-A^b- and 80 LLOp:I-A^b-specific CD4$^+$ T cells in the spleen and lymph nodes, most of which were CD44^{low} as expected for naïve cells (Fig. 1A). No CD4$^+$ T cells bound both tetramers and less than 5 CD8$^+$ T cells per mouse bound either tetramer, demonstrating that tetramer binding was TCR-specific. TCR Vα2$^+$ cells were under represented in the 2W:I-A^b-specific naive populations but over represented in the LLOp:I-A^b-specific naive populations in wild-type and CD28-deficient mice (Fig. 1B). The fact that 2W:I-A^b- and LLOp:I-A^b-specific naive populations had similar sizes and compositions in wild-type and CD28-deficient mice indicated that CD28 deficiency did not grossly alter the T cell repertoire.

Wild-type and CD28-deficient mice were then infected intravenously with Lm-2W bacteria to assess the role of CD28 in the activation of naive T cells *in vivo*. The 2W:I-A^b-specific cells in each group increased comparably over the first 3 days after Lm-2W infection (Fig. 2A). However, by day 4 this population was 10-times smaller in CD28-deficient mice than in wild-type mice, a difference that was maintained at the peak on day 5. The 2W:I-A^b-specific populations in CD28-deficient and wild-type mice then contracted between days 5 and 20 with a half-life of about 2 days and fell to 10% of their respective maximum values. The 10-fold difference between the two groups was then maintained after day 20 as both populations declined slowly during the memory phase with a half-life of ~50 days (Fig. 2A). LLOp:I-A^b-specific T cells also expanded about 10-fold less well in CD28-deficient than in B6 mice, a difference that was maintained 20 days post infection Fig. 2B). Thus, CD28 deficiency impaired the extent of CD4$^+$ T cell expansion but did not alter survival during the contraction or memory phases.

CD28 is necessary to sustain cell cycle activity of p:MHCII-specific CD4$^+$ T cells *in vivo*

CD28 signals enhance cell cycle entry and G_1 to S phase cell cycle progression of CD4$^+$ T cells *in vitro* (51–55) and sustain proliferation of monoclonal T cells *in vivo* (56, 57). DNA replication was measured to determine if CD28 deficiency impaired cell cycle activity in polyclonal p:MHCII-specific CD4$^+$ T cells during infection (Fig. 3A). All naïve CD44^{low} 2W:I-A^b-specific T cells from uninfected wild-type and CD28-deficient mice were in G_0/G_1. Similar numbers of 2W:I-A^b-specific T cells progressed to S and G_2/M in both groups on day 2. The proportion of cells in S and G_2/M in both groups peaked on day 3, but CD28-deficient mice had fewer cells in S and G_2/M than controls. By day 4, both groups were

returning to G_0/G_1, with CD28-deficient mice having fewer cycling cells. Thus, CD28 was not needed for entry into S and G_2/M in the early stages of clonal expansion but was required for maintaining cell cycle activity.

To further test whether the requirement of CD28 for sustained T cell cycling was cell-intrinsic, polyclonal $CD4^+$ T cells from the spleen and lymph nodes of wild-type or CD28-deficient mice were labeled with CFSE and transferred into congenic recipients, which were then infected with Lm-2W bacteria. About 100 donor-derived wild-type and CD28-deficient 2W:I-A^b-specific T cells were detected in uninfected recipients, and these were $CFSE^{high}$ (Fig 3B) as expected for quiescent naïve cells. By day 3, both 2W:I-A^b-specific wild-type and CD28-deficient donor T cells had diluted CFSE similarly and expanded about 4-fold (Fig. 3B). By day 5, most of the wild-type T cells had diluted CFSE beyond the limit of detection. In contrast, most CD28-deficient T cells had not diluted CFSE beyond the levels achieved by day 3. The transferred wild-type T cells expanded about 130-fold above the starting number by day 5, while the CD28-deficient T cells increased only 7-fold (Fig 3B). Thus, CD28 was necessary to sustain, but not initiate $CD4^+$ T cell proliferation in response to *L. monocytogenes* infection.

The PYAP and Y170F motifs of CD28 are dispensable for $CD4^+$ T cell clonal expansion in response to *L. monocytogenes* infection

We next attempted to identify the regions of the CD28 cytoplasmic tail that produced these biological effects. This was done using mixed hematopoietic cell chimeras produced by transplanting lethally irradiated mice with equal numbers of wild-type and CD28-deficient bone marrow cells (Fig 4A). These chimeras contained similar numbers of wild-type and CD28-deficient 2W:I-A^b-specific naive $CD4^+$ T cells (Fig. 4B). In contrast, the wild-type 2W:I-A^b-specific $CD4^+$ T cells expanded 50-fold more than the CD28-deficient cells following Lm-2W infection (Fig 4B).

The role of the cytoplasmic tail was tested in mixed chimeras containing wild-type T cells and *Cd28*$^{-/-}$ T cells expressing full-length or cytoplasmic tail-deficient (Tail-less) *Cd28* transgenes. The 2W:I-A^b-specific $CD4^+$ T cells with tailless CD28 expanded about 10 times less than the cells with full-length CD28 (Fig. 4C). Remarkably, however, 2W:I-A^b-specific $CD4^+$ T cells with a mutated C-terminal PYAP motif (AYAA), an SH2 domain-binding YMNM motif (Y170F), or both mutations expanded to the same extent as the wild-type $CD4^+$ T cells after Lm-2W infection (Fig. 4D – F). Thus, the cytoplasmic tail, but neither the PYAP nor the YMNM motifs within the tail were required for the *in vivo* effects of CD28 on clonal expansion after this infection.

It was possible that these negative results were related to the involvement of costimulatory receptors other than CD28, the ligands for which are induced by infection. This possibility was tested by assessing the responsiveness of the CD28-deficient T cells following injection of peptide without an adjuvant. As shown in Fig. 4G, injection of 2W peptide alone induced expansion of wild-type 2W:I-A^b-specific T cells, but at a level that was about 40-fold lower than that induced by Lm-2W infection. The expansion of CD28-deficient 2W:I-A^b-specific T cells after injection of 2W peptide alone was 8-fold lower than that of wild-type cells. The expansions of 2W:I-A^b-specific $CD4^+$ T cells with mutated PYAP or YMNM motifs were also lower than that of wild-type cells but only by 2-fold. These results indicate that the PYAP and YMNM sites in the cytoplasmic tail of CD28 transduce signals in polyclonal p:MHCII-specific $CD4^+$ T cells under conditions of minimal inflammation.

CD28 deficiency phenotypically resembles T cell-intrinsic NFκB signaling deficiency during response to *L. monocytogenes* infection

The perplexing finding that neither of the suspected motifs within the tail were required for the *in vivo* effects of CD28 led us to investigate whether NFκB signaling was involved. This was the case as evidenced by the finding that CD28-deficient 2W:I-A^b- and LLOp:I-A^b-specific T cells did not induce Bcl-x_L, an NFκB-regulated gene product (17, 18), 3 days after Lm-2W infection like control cells (Fig. 5A). These findings suggested that signals from CD28 contribute to activation of NFκB in this setting. If so, then loss of NFκB signaling would be expected to produce the same defects in T cell activation as CD28 deficiency. This possibility was tested in radiation bone marrow chimeras containing wild-type and *Card11*$^{-/-}$ T cells lacking the CARMA1 component of the NFkB signaling pathway. Like CD28-deficient cells, CARMA1-deficient 2W:I-A^b-specific T cells began to expand normally on day 3 after infection but did not continue to expand to day 5 when these T cells exhibited a 40-fold defect compared to wild-type cells (Fig. 5B). Similary, CARMA1-deficient failed to induce Bcl-x_L (Fig 5B) like CD28-deficient cells. PKCθ- and NFκB1/c-Rel-deficient 2W:I-A^b-specific $CD4^+$ T cells had similar clonal expansion defects (Fig. 5C and D). These results show that the expansion defect of CD28-deficient cells resembles that of NFκB signaling-deficient cells.

CD28 signaling increases antigen-dependent nuclear translocation of RelA *in vivo* independently of the PYAP and YMNM motifs

To determine if CD28 signaling indeed enhanced NFκB activation *in vivo*, we used an image scanning flow cytometer to measure nuclear translocation of RelA in $CD4^+$ T cells responding to antigen *in vivo*. We chose to focus on RelA because this NFκB isoform can dimerize with p50 or c-Rel in T cells (58), translocates into the nucleus upon TCR plus CD28 stimulation, and is a component of a protein complex that can bind the CD28 response element consensus sequence (59). $CD4^+$ T cells from wild-type or CD28-deficient OVA peptide:I-A^b-specific OT-II TCR transgenic mice were transferred into normal mice, which were then injected intravenously with LPS to induce CD80 and CD86 on APC, then with OVA peptide (60, 61) (Fig. 6A). RelA was in the cytoplasm of wild-type and CD28-deficient OT-II cells in recipient mice injected with LPS alone (Fig. 6). In contrast, RelA translocated to the nucleus in OT-II cells 20 minutes after injection of OVA peptide, and this translocation was significantly greater in wild-type than in CD28-deficient cells (Fig. 6C). Additionally, OT-II expressing CD28 molecules with mutated PYAP or YMNM sites showed the same amount of peptide-induced RelA translocation as wild-type cells (Fig. 6C). These data demonstrate that CD28 signaling is required for optimal TCR-induced activation of RelA *in vivo* through a pathway that does not involve the YMNM or PYAP sites.

Discussion

Our results show that the major effect of CD28 signaling on polyclonal p:MHCII-specific T cells responding to an infection was sustained effector cell proliferation. It was surprising to find that CD28-deficient T cells began proliferating *in vivo* at the same rate as wild-type T cells given the many reports that CD28 enhances the production of the early T cell growth factor IL-2. However, this result is less surprising considering evidence that IL-2 is not required for $CD4^+$ T cell proliferation *in vivo* (60). It is possible that CD28 maintains effector cell proliferation indirectly by sustaining the production of a lymphokine other than IL-2 (62) or by directly transducing signals that promote cell cycle progression (51, 53).

It has been reported that CD28 does not influence *in vitro* T cell proliferation, but rather promotes clonal expansion by opposing apoptosis through induction of Bcl-x_L (10). This was proposed to be an indirect effect of OX40, which promotes memory T cell formation

and expression of Bcl-x_L and is induced in a CD28-dependent fashion (63). In contrast, we found that the polyclonal p:MHCII-specific effector cells that were formed in CD28-deficient mice did not undergo an exaggerated contraction phase and produced memory cells at the expected frequency. This conclusion is supported by the observation of Dahl et al. that over expression of Bcl-x_L failed to restore the clonal expansion of CD28-deficient T cells *in vivo* (64). Therefore, the *in vivo* results indicate that CD28 enhances memory cell generation by sustaining the proliferation of the effector cell population from which memory cells are derived.

It was surprising to find that mutations of the YMNM site had no effect on the production of effector and memory T cells after bacterial infection. The YMNM site has been shown to bind to PI3K, a key molecule in the activation of multiple signaling pathways that regulate cellular metabolism (AKT/mTOR), the immunological synapse (PKCθ), and transcription of genes involved in T cell proliferation and survival (Bcl10/Carma1/Malt1/NFκB) (12, 13) (12, 14–16)(17–19). Our results are consistent, however, with reports showing that disruption of the YMNM motif and prevention of PI3K binding and phosphorylation of Akt had no effect on IL-2 production *in vitro* or the induction of T cell-dependent airway inflammation or experimental allergic encephalomyelitis *in vivo* (23, 24). Our findings extend this work by documenting that the YMNM site is dispensable for the infection-induced proliferation of polyclonal p:MHCII-specific polyclonal $CD4^+$ T cells. Notably, both the PYAP and YMNM sites played a role in T cell expansion induced by peptide without adjuvant, perhaps because fewer costimulatory ligands other than CD80 and CD86 are induced in this case than by infection. It was even more surprising to find that mutations in the PYAP site had no effect on the production of effector and memory T cells after bacterial infection. This site is involved of activation of PDK1 and PKCθ and its disruption impairs *in vivo* T cell functions such as promotion of antibody production and induction of experimental allergic encephalomyelitis. Our observation that p:MHCII-specific $CD4^+$ T cells failed proliferate to the same extent as wild-type cells after injection of peptide alone indicates defective clonal expansion could explain the aforementioned defects. However, the finding that PYAP mutant p:MHCII-specific $CD4^+$ T cells underwent normal clonal expansion under the more inflammatory condition of bacterial infection shows that this site is not critical for T cell proliferation in all immune responses.

Our finding that CD28-deficient T cells did not translocate RelA to the nucleus as well as wild-type T cells following *in vivo* p:MHCII stimulation is consistent with the idea that canonical NFκB activation is a critical component of the CD28 signal that sustains T cell proliferation. Remarkably, however, RelA translocation could not be attributed to the YMNM or PYAP sites, both of which have been implicated in NFκB signaling in some cases. It is therefore possible that CD28 activates the NFκB signaling cascade without recruiting PI3K of other effectors to the YMNM or PYAP sites in its cytoplasmic tail. It is still possible, however, that CD28 triggers NFκB signaling through PI3K without recruiting it to the cytoplasmic tail as suggested by Garçon et al (65). Another possibility is that the tyrosine within the PYAP motif, which is required for PKCθ focusing within the immunological synapse (26), is necessary for CD28-dependent NFκB activation *in vivo*. In any case, our results point out the need to study CD28 signaling in relevant *in vivo* models and suggest that there is more to be learned about how the cytoplasmic tail transduces signals.

Acknowledgments

Grant Support: This work was supported by grants from the US National Institutes of Health, R37-AI027998, R01AI39614, and R01-AI66016 (M.K.J.), T32-AI07313 (A.J.P.), and T32-CA9138 (M.P.), a Frieda M. Kunze Fellowship from the Minnesota Medical Foundation (A.J.P.), and an American Heart Association Fellowship (H.H.C.).

We thank Dr. D. Mueller for reviewing the manuscript, Drs. A. Beg, M. Farrar, S. Gerondakis, D. Littman, and A. Singer for providing mice, Dr. B. Burbach and T. Martin for guidance on scanning flow cytometry, G. Hart and J. Linehan for help with bone marrow chimeras, and J. Walter, A. Schmidt, M. Priess, and R. Speier for technical assistance.

Abbreviations

PI3K	phosphatidylinositol 3-kinase
PKCθ	protein kinase C θ
CARMA1	CARD-containing MAGUK protein 1
NFκB	nuclear factor κB
OVA	chicken ovalbumin
LLO	listeriolysin O

References

1. Jenkins MK, Khoruts A, Ingulli E, Mueller DL, McSorley SJ, Reinhardt RL, Itano A, Pape KA. In vivo activation of antigen-specific CD4 T cells. Annu Rev Immunol. 2001; 19:23–45. [PubMed: 11244029]
2. Janeway CA Jr, Medzhitov R. Innate immune recognition. Annu Rev Immunol. 2002; 20:197–216. [PubMed: 11861602]
3. Ahmed R, Gray D. Immunological memory and protective immunity: understanding their relation. Science. 1996; 272:54–60. [PubMed: 8600537]
4. Ferguson SE, Han S, Kelsoe G, Thompson CB. CD28 is required for germinal center formation. J Immunol. 1996; 156:4576–4581. [PubMed: 8648099]
5. McSorley SJ, Jenkins MK. Antibody is required for protection against virulent but not attenuated Salmonella enterica serovar typhimurium. Infect Immun. 2000; 68:3344–3348. [PubMed: 10816483]
6. Lindstein T, June CH, Ledbetter JA, Stella G, Thompson CB. Regulation of lymphokine messenger RNA stability by a surface-mediated T cell activation pathway. Science. 1989; 244:339–343. [PubMed: 2540528]
7. Umlauf SW, Beverly B, Lantz O, Schwartz RH. Regulation of interleukin 2 gene expression by CD28 costimulation in mouse T-cell clones: both nuclear and cytoplasmic RNAs are regulated with complex kinetics. Mol Cell Biol. 1995; 15:3197–3205. [PubMed: 7539104]
8. Frauwirth KA, Riley JL, Harris MH, Parry RV, Rathmell JC, Plas DR, Elstrom RL, June CH, Thompson CB. The CD28 signaling pathway regulates glucose metabolism. Immunity. 2002; 16:769–777. [PubMed: 12121659]
9. Boise LH, Minn AJ, Noel PJ, June CH, Accavitti MA, Lindsten T, Thompson CB. CD28 costimulation can promote T cell survival by enhancing the expression of Bcl-XL. Immunity. 1995; 3:87–98. [PubMed: 7621080]
10. Sperling AI, Auger JA, Ehst BD, Rulifson IC, Thompson CB, Bluestone JA. CD28/B7 interactions deliver a unique signal to naive T cells that regulates cell survival but not early proliferation. J Immunol. 1996; 157:3909–3917. [PubMed: 8892622]
11. Pages F, Ragueneau M, Rottapel R, Truneh A, Nunes J, Imbert J, Olive D. Binding of phosphatidylinositol-3-OH kinase to CD28 is required for T-cell signalling. Nature. 1994; 369:327–329. [PubMed: 8183372]
12. Sanchez-Lockhart M, Marin E, Graf B, Abe R, Harada Y, Sedwick CE, Miller J. Cutting edge: CD28-mediated transcriptional and posttranscriptional regulation of IL-2 expression are controlled through different signaling pathways. J Immunol. 2004; 173:7120–7124. [PubMed: 15585831]
13. Yokosuka T, Kobayashi W, Sakata-Sogawa K, Takamatsu M, Hashimoto-Tane A, Dustin ML, Tokunaga M, Saito T. Spatiotemporal regulation of T cell costimulation by TCR-CD28

microclusters and protein kinase C theta translocation. Immunity. 2008; 29:589–601. [PubMed: 18848472]

14. Park SG, Schulze-Luehrman J, Hayden MS, Hashimoto N, Ogawa W, Kasuga M, Ghosh S. The kinase PDK1 integrates T cell antigen receptor and CD28 coreceptor signaling to induce NF-kappaB and activate T cells. Nat Immunol. 2009; 10:158–166. [PubMed: 19122654]
15. Narayan P, Holt B, Tosti R, Kane LP. CARMA1 is required for Akt-mediated NF-kappaB activation in T cells. Mol Cell Biol. 2006; 26:2327–2336. [PubMed: 16508008]
16. Jones RG, Parsons M, Bonnard M, Chan VS, Yeh WC, Woodgett JR, Ohashi PS. Protein kinase B regulates T lymphocyte survival, nuclear factor kappaB activation, and Bcl-X(L) levels in vivo. J Exp Med. 2000; 191:1721–1734. [PubMed: 10811865]
17. Khoshnan A, Tindell C, Laux I, Bae D, Bennett B, Nel AE. The NF-kappa B cascade is important in Bcl-xL expression and for the anti-apoptotic effects of the CD28 receptor in primary human CD4+ lymphocytes. J Immunol. 2000; 165:1743–1754. [PubMed: 10925251]
18. Chen C, Edelstein LC, Gelinas C. The Rel/NF-kappaB family directly activates expression of the apoptosis inhibitor Bcl-x(L). Mol Cell Biol. 2000; 20:2687–2695. [PubMed: 10733571]
19. Burr JS, Savage ND, Messah GE, Kimzey SL, Shaw AS, Arch RH, Green JM. Cutting edge: distinct motifs within CD28 regulate T cell proliferation and induction of Bcl-XL. J Immunol. 2001; 166:5331–5335. [PubMed: 11313368]
20. Rathmell JC, Elstrom RL, Cinalli RM, Thompson CB. Activated Akt promotes increased resting T cell size, CD28-independent T cell growth, and development of autoimmunity and lymphoma. Eur J Immunol. 2003; 33:2223–2232. [PubMed: 12884297]
21. Song J, Salek-Ardakani S, So T, Croft M. The kinases aurora B and mTOR regulate the G1-S cell cycle progression of T lymphocytes. Nat Immunol. 2007; 8:64–73. [PubMed: 17128276]
22. Edinger AL, Thompson CB. Akt maintains cell size and survival by increasing mTOR-dependent nutrient uptake. Mol Biol Cell. 2002; 13:2276–2288. [PubMed: 12134068]
23. Okkenhaug K, Wu L, Garza KM, La Rose J, Khoo W, Odermatt B, Mak TW, Ohashi PS, Rottapel R. A point mutation in CD28 distinguishes proliferative signals from survival signals. Nat Immunol. 2001; 2:325–332. [PubMed: 11276203]
24. Dodson LF, Boomer JS, Deppong CM, Shah DD, Sim J, Bricker TL, Russell JH, Green JM. Targeted knock-in mice expressing mutations of CD28 reveal an essential pathway for costimulation. Mol Cell Biol. 2009; 29:3710–3721. [PubMed: 19398586]
25. Friend LD, Shah DD, Deppong C, Lin J, Bricker TL, Juehne TI, Rose CM, Green JM. A dose-dependent requirement for the proline motif of CD28 in cellular and humoral immunity revealed by a targeted knockin mutant. J Exp Med. 2006; 203:2121–2133. [PubMed: 16908623]
26. Sanchez-Lockhart M, Graf B, Miller J. Signals and sequences that control CD28 localization to the central region of the immunological synapse. J Immunol. 2008; 181:7639–7648. [PubMed: 19017952]
27. Wulfing C, Davis MM. A receptor/cytoskeletal movement triggered by costimulation during T cell activation. Science. 1998; 282:2266–2269. [PubMed: 9856952]
28. Wulfing C, Sumen C, Sjaastad MD, Wu LC, Dustin ML, Davis MM. Costimulation and endogenous MHC ligands contribute to T cell recognition. Nat Immunol. 2002; 3:42–47. [PubMed: 11731799]
29. Viola A, Schroeder S, Sakakibara Y, Lanzavecchia A. T lymphocyte costimulation mediated by reorganization of membrane microdomains. Science. 1999; 283:680–682. [PubMed: 9924026]
30. Andres PG, Howland KC, Dresnek D, Edmondson S, Abbas AK, Krummel MF. CD28 signals in the immature immunological synapse. J Immunol. 2004; 172:5880–5886. [PubMed: 15128767]
31. Tavano R, Contento RL, Baranda SJ, Soligo M, Tuosto L, Manes S, Viola A. CD28 interaction with filamin-A controls lipid raft accumulation at the T-cell immunological synapse. Nat Cell Biol. 2006; 8:1270–1276. [PubMed: 17060905]
32. Holdorf AD, Green JM, Levin SD, Denny MF, Straus DB, Link V, Changelian PS, Allen PM, Shaw AS. Proline residues in CD28 and the Src homology (SH)3 domain of Lck are required for T cell costimulation. J Exp Med. 1999; 190:375–384. [PubMed: 10430626]
33. Holdorf AD, Lee KH, Burack WR, Allen PM, Shaw AS. Regulation of Lck activity by CD4 and CD28 in the immunological synapse. Nat Immunol. 2002; 3:259–264. [PubMed: 11828322]

34. Hataye J, Moon JJ, Khoruts A, Reilly C, Jenkins MK. Naive and memory CD4+ T cell survival controlled by clonal abundance. Science. 2006; 312:114–116. [PubMed: 16513943]

35. Shahinian A, Pfeffer K, Lee KP, Kundig TM, Kishihara K, Wakeham A, Kawai K, Ohashi PS, Thompson CB, Mak TW. Differential T cell costimulatory requirements in CD28-deficient mice. Science. 1993; 261:609–612. [PubMed: 7688139]

36. Mombaerts P, Iacomini J, Johnson RS, Herrup K, Tonegawa S, Papaioannou VE. RAG-1-deficient mice have no mature B and T lymphocytes. Cell. 1992; 68:869–877. [PubMed: 1547488]

37. Tai X, Cowan M, Feigenbaum L, Singer A. CD28 costimulation of developing thymocytes induces Foxp3 expression and regulatory T cell differentiation independently of interleukin 2. Nat Immunol. 2005; 6:152–162. [PubMed: 15640801]

38. Sun Z, Arendt CW, Ellmeier W, Schaeffer EM, Sunshine MJ, Gandhi L, Annes J, Petrzilka D, Kupfer A, Schwartzberg PL, Littman DR. PKC-theta is required for TCR-induced NF-kappaB activation in mature but not immature T lymphocytes. Nature. 2000; 404:402–407. [PubMed: 10746729]

39. Sha WC, Liou HC, Tuomanen EI, Baltimore D. Targeted disruption of the p50 subunit of NF-kappa B leads to multifocal defects in immune responses. Cell. 1995; 80:321–330. [PubMed: 7834752]

40. Kontgen F, Grumont RJ, Strasser A, Metcalf D, Li R, Tarlinton D, Gerondakis S. Mice lacking the c-rel proto-oncogene exhibit defects in lymphocyte proliferation, humoral immunity, and interleukin-2 expression. Genes Dev. 1995; 9:1965–1977. [PubMed: 7649478]

41. Egawa T, Albrecht B, Favier B, Sunshine MJ, Mirchandani K, O'Brien W, Thome M, Littman DR. Requirement for CARMA1 in antigen receptor-induced NF-kappa B activation and lymphocyte proliferation. Curr Biol. 2003; 13:1252–1258. [PubMed: 12867038]

42. Ertelt JM, Rowe JH, Johanns TM, Lai JC, McLachlan JB, Way SS. Selective priming and expansion of antigen-specific Foxp3-CD4+ T cells during Listeria monocytogenes infection. J Immunol. 2009; 182:3032–3038. [PubMed: 19234199]

43. Moon JJ, Chu HH, Pepper M, McSorley SJ, Jameson SC, Kedl RM, Jenkins MK. Naive CD4(+) T cell frequency varies for different epitopes and predicts repertoire diversity and response magnitude. Immunity. 2007; 27:203–213. [PubMed: 17707129]

44. Moon JJ, Chu HH, Hataye J, Pagan AJ, Pepper M, McLachlan JB, Zell T, Jenkins MK. Tracking epitope-specific T cells. Nat Protoc. 2009; 4:565–581. [PubMed: 19373228]

45. Quah BJ, Warren HS, Parish CR. Monitoring lymphocyte proliferation in vitro and in vivo with the intracellular fluorescent dye carboxyfluorescein diacetate succinimidyl ester. Nat Protoc. 2007; 2:2049–2056. [PubMed: 17853860]

46. Pepper M, Pagan AJ, Igyarto BZ, Taylor JJ, Jenkins MK. Opposing Signals from the Bcl6 Transcription Factor and the Interleukin-2 Receptor Generate T Helper 1 Central and Effector Memory Cells. Immunity. 2011; 35:583–95. [PubMed: 22018468]

47. Medeiros RB, Burbach BJ, Mueller KL, Srivastava R, Moon JJ, Highfill S, Peterson EJ, Shimizu Y. Regulation of NF-kappaB activation in T cells via association of the adapter proteins ADAP and CARMA1. Science. 2007; 316:754–758. [PubMed: 17478723]

48. Portnoy DA, Auerbuch V, Glomski IJ. The cell biology of Listeria monocytogenes infection: the intersection of bacterial pathogenesis and cell-mediated immunity. J Cell Biol. 2002; 158:409–414. [PubMed: 12163465]

49. Rees W, Bender J, Teague TK, Kedl RM, Crawford F, Marrack P, Kappler J. An inverse relationship between T cell receptor affinity and antigen dose during CD4(+) T cell responses in vivo and in vitro. Proc Natl Acad Sci U S A. 1999; 96:9781–9786. [PubMed: 10449771]

50. Geginat G, Schenk S, Skoberne M, Goebel W, Hof H. A novel approach of direct ex vivo epitope mapping identifies dominant and subdominant CD4 and CD8 T cell epitopes from Listeria monocytogenes. J Immunol. 2001; 166:1877–1884. [PubMed: 11160235]

51. Appleman LJ, van Puijenbroek AA, Shu KM, Nadler LM, Boussiotis VA. CD28 costimulation mediates down-regulation of p27kip1 and cell cycle progression by activation of the PI3K/PKB signaling pathway in primary human T cells. J Immunol. 2002; 168:2729–2736. [PubMed: 11884439]

52. Bonnevier JL, Mueller DL. Cutting edge: B7/CD28 interactions regulate cell cycle progression independent of the strength of TCR signaling. J Immunol. 2002; 169:6659–6663. [PubMed: 12471093]

53. Bonnevier JL, Yarke CA, Mueller DL. Sustained B7/CD28 interactions and resultant phosphatidylinositol 3-kinase activity maintain G1-->S phase transitions at an optimal rate. Eur J Immunol. 2006; 36:1583–1597. [PubMed: 16703564]

54. Iezzi G, Karjalainen K, Lanzavecchia A. The duration of antigenic stimulation determines the fate of naive and effector T cells. Immunity. 1998; 8:89–95. [PubMed: 9462514]

55. Wells AD, Gudmundsdottir H, Turka LA. Following the fate of individual T cells throughout activation and clonal expansion. Signals from T cell receptor and CD28 differentially regulate the induction and duration of a proliferative response. J Clin Invest. 1997; 100:3173–3183. [PubMed: 9399965]

56. Gudmundsdottir H, Wells AD, Turka LA. Dynamics and requirements of T cell clonal expansion in vivo at the single-cell level: effector function is linked to proliferative capacity. J Immunol. 1999; 162:5212–5223. [PubMed: 10227995]

57. Khoruts A, Osness RE, Jenkins MK. IL-1 acts on antigen-presenting cells to enhance the in vivo proliferation of antigen-stimulated naive CD4 T cells via a CD28-dependent mechanism that does not involve increased expression of CD28 ligands. Eur J Immunol. 2004; 34:1085–1090. [PubMed: 15048719]

58. Harhaj EW, Maggirwar SB, Good L, Sun SC. CD28 mediates a potent costimulatory signal for rapid degradation of IkappaBbeta which is associated with accelerated activation of various NF-kappaB/Rel heterodimers. Mol Cell Biol. 1996; 16:6736–6743. [PubMed: 8943328]

59. Ghosh P, Tan TH, Rice NR, Sica A, Young HA. The interleukin 2 CD28-responsive complex contains at least three members of the NF kappa B family: c-Rel, p50, and p65. Proc Natl Acad Sci U S A. 1993; 90:1696–1700. [PubMed: 8383323]

60. Khoruts A, Mondino A, Pape KA, Reiner SL, Jenkins MK. A natural immunological adjuvant enhances T cell clonal expansion through a CD28-dependent, interleukin (IL)-2-independent mechanism. J Exp Med. 1998; 187:225–236. [PubMed: 9432980]

61. De Smedt T, Pajak B, Muraille E, Lespagnard L, Heinen E, De Baetselier P, Urbain J, Leo O, Moser M. Regulation of dendritic cell numbers and maturation by lipopolysaccharide in vivo. J Exp Med. 1996; 184:1413–1424. [PubMed: 8879213]

62. Boulougouris G, McLeod JD, Patel YI, Ellwood CN, Walker LS, Sansom DM. IL-2-independent activation and proliferation in human T cells induced by CD28. J Immunol. 1999; 163:1809–1816. [PubMed: 10438913]

63. Rogers PR, Song J, Gramaglia I, Killeen N, Croft M. OX40 promotes Bcl-xL and Bcl-2 expression and is essential for long-term survival of CD4 T cells. Immunity. 2001; 15:445–455. [PubMed: 11567634]

64. Dahl AM, Klein C, Andres PG, London CA, Lodge MP, Mulligan RC, Abbas AK. Expression of bcl-X(L) restores cell survival, but not proliferation off effector differentiation, in CD28-deficient T lymphocytes. J Exp Med. 2000; 191:2031–2038. [PubMed: 10859328]

65. Garcon F, Patton DT, Emery JL, Hirsch E, Rottapel R, Sasaki T, Okkenhaug K. CD28 provides T-cell costimulation and enhances PI3K activity at the immune synapse independently of its capacity to interact with the p85/p110 heterodimer. Blood. 2008; 111:1464–1471. [PubMed: 18006698]

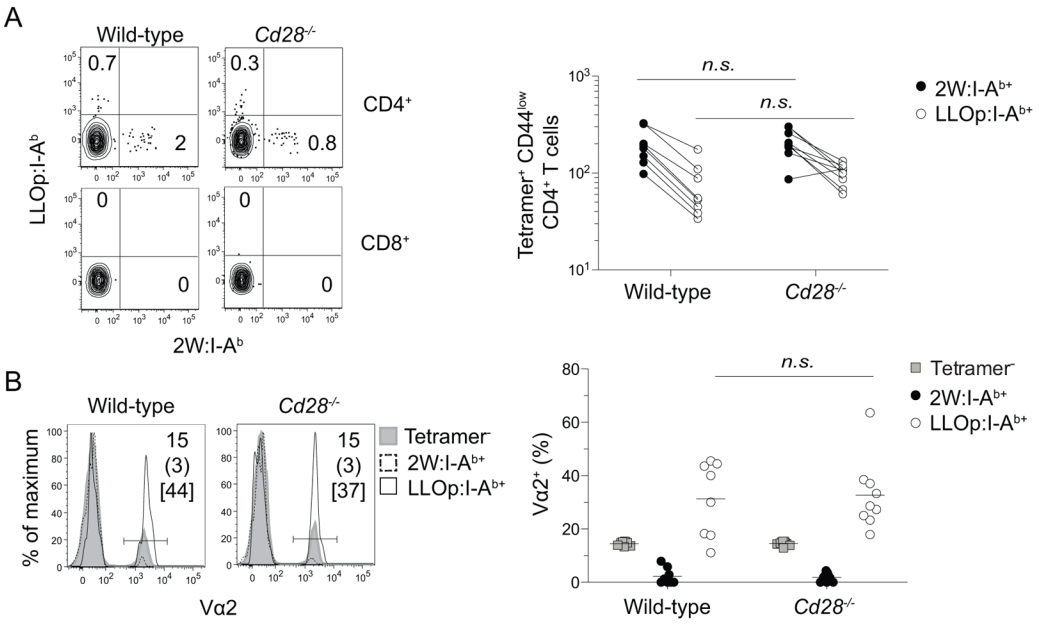

Figure 1. Detection of naive p:MHCII-specific CD4$^+$ T cells in wild-type and CD28-deficient mice

2W:I-A^{b+} and LLOp:I-A^{b+} T cells were magnetically enriched from pooled spleen and lymph nodes and visualized by flow cytometry. (A) Flow cytometry plots of 2W:I-A^b and LLOp:I-A^b tetramer-staining of CD3$^+$ non-T lineage marker$^-$ CD4$^+$ or CD8$^+$ T cells (left), and enumeration of tetramer-stained CD4$^+$ T cells in wild-type and CD28-deficient mice (right). Numbers on the plots depict the percentages of 2W:I-A^{b+} and LLOp:I-A^b within the enriched CD4$^+$ or CD8$^+$ T cells. Lines on the graph connect the number of 2W:I-A^{b+} and LLOp:I-A^{b+} T cells in individual mice. (B) Histograms (left) of Vα2 staining on 2W:I-A^{b+}, LLOp:I-A^{b+}, and tetramer$^-$ T cells, and the percentage of Vα2$^+$ cells among these three cell types (right). Numbers in histograms show the percentage of Vα2$^+$ cells in tetramer$^-$ T cells (top), 2W:I-A^{b+} T cells (middle), and LLOp:I-A^{b+} T cells (bbottom). Horizontal lines on the plot indicate mean values, and each symbol depicts a value from an individual mouse. Groups were compared with a two-tailed Student's *t* test. *n.s.,* not significant, $p > 0.05$. Pooled data from two (A) or four (B) independent experiments are shown.

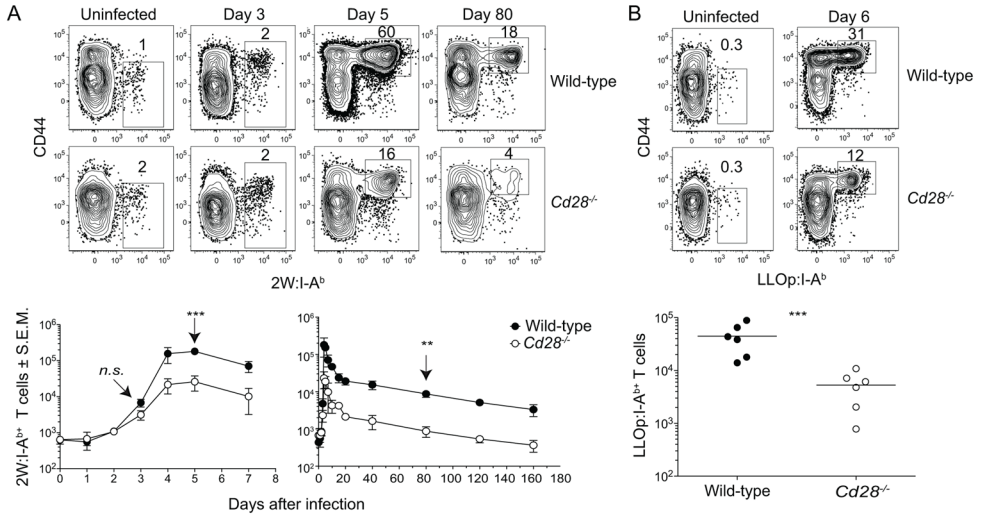

Figure 2. Kinetics of primary CD4$^+$ T cell response to *L. monocytogenes* in wild-type and CD28-deficient mice

2W:I-A^{b+} or LLOp:I-A^{b+} T cells were magnetically enriched from wild-type and CD28-deficient mice infected intravenously with Lm-2W.. (A) and (B) Flow cytometry plots of (A) 2W:I-A^b or (B) LLOp:I-A^b versus CD44 staining on CD4$^+$ T cells from wild-type or CD28-deficient mice (top) with graphs depicting the nmean number (n ≥ 3) of (A) 2W:I-A^{b+} or (B) LLOp:I-A^{b+} T cells (bottom). A two-tailed Student's *t* test on the $\log_{10}$ values of each group at the indicated time points (arrow) was used to determine statistical significance, *n.s.,* not significant, $p > 0.05$; ** $p < 0.01$, *** $p < 0.001$. Pooled data from six (A) or two (B) independent experiments are shown.

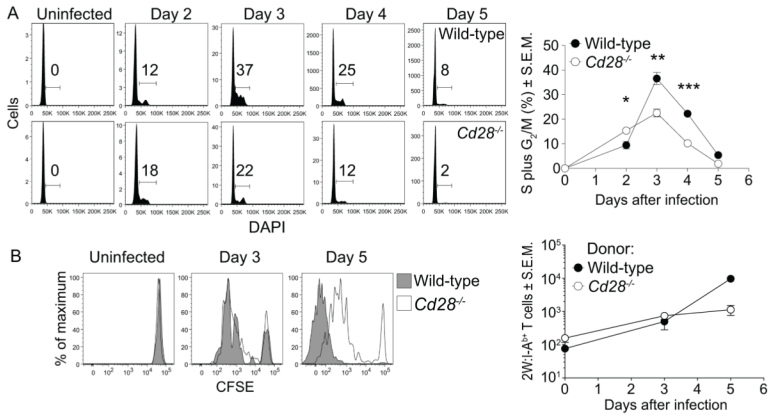

Figure 3. CD28 is required to sustain but not initiate CD4$^+$ T cell proliferation *in vivo.*

(*A*) Histograms of DAPI staining on 2W:I-A^{b+} T cells from wild-type or CD28-deficient mice infected with Lm-2W bacteria (left). Gates show the percentages of cells in S plus G_2/M phases of the cell cycle. Mean percentage (n ≥ 3) of 2W:I-A^{b+} T cells in S plus G_2/M (right). A two-tailed Student's *t* test was used to identify statistical differences between groups, * $p < 0.05$; ** $p < 0.01$, *** $p < 0.001$. (*B*) Histograms of CFSE in 2W:I-A^{b+} T cells from CD90.2$^+$ wild-type or CD28-deficient CD4$^+$ T cells in CD90.1$^+$ wild-type recipients that were subsequently infected with Lm-2W (left) with the mean number (2 – 4 mice per time point) of donor-derived wild-type or CD28-deficient 2W:I-A^{b+} T cells (right). Each graph shows pooled data from three independent experiments.

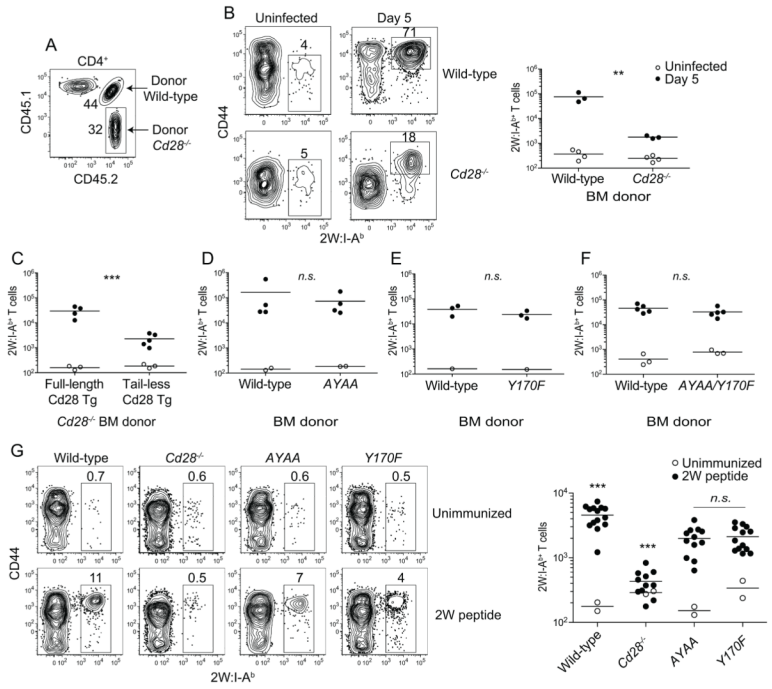

Figure 4. The PYAP and YMNM motifs of CD28 are dispensable for CD28-dependent CD4$^+$ T cell clonal expansion in response to *L. monocytogenes* infection

(A) Flow cytometry plot showing gates used to identify wild-type and CD28-deficient CD4$^+$ T cells in a 2W:I-A^b tetramer-enriched sample from a radiation bone marrow chimeric mouse. Numbers indicate the percentage of donor wild-type or CD28-deficient CD4$^+$ T cells in the enriched sample. (B) Flow cytometry plots of 2W:I-A^b versus CD44 on donor-derived wild-type or CD28-deficient CD4$^+$ T cells from uninfected or day 5 Lm-2W infected mice (left). (B right plot - F) Numbers of wild-type and CD28 mutant 2W:I-A^{b+} T cells in uninfected and day 5 Lm-2W infected mice. (G) Flow cytometry plots of 2W:I-A^b versus CD44 on CD4$^+$ T cells from the spleens of wild-type or CD28 mutant mice (left) and absolute numbers of 2W:I-A^{b+} T cells in unimmunized mice (open circles) or mice that had been injected intravenously 5 days earlier with 2W peptide without the addition of any adjuvant (filled circles). A two-tailed Student's *t* test was used to compare the $\log_{10}$ values of Lm-2W infected groups and a one-way ANOVA with Bonferroni post-test was used to compare the $\log_{10}$ values of peptide-immunized groups, *n.s.* $p > 0.05$; ** $p < 0.01$, *** $p < 0.001$. All groups were compared to each other. Asterisks above wild-type and *Cd28*$^{-/-}$ samples indicate that all comparisons involving these groups revealed statistically significant differences. Data are from one to five independent experiments.

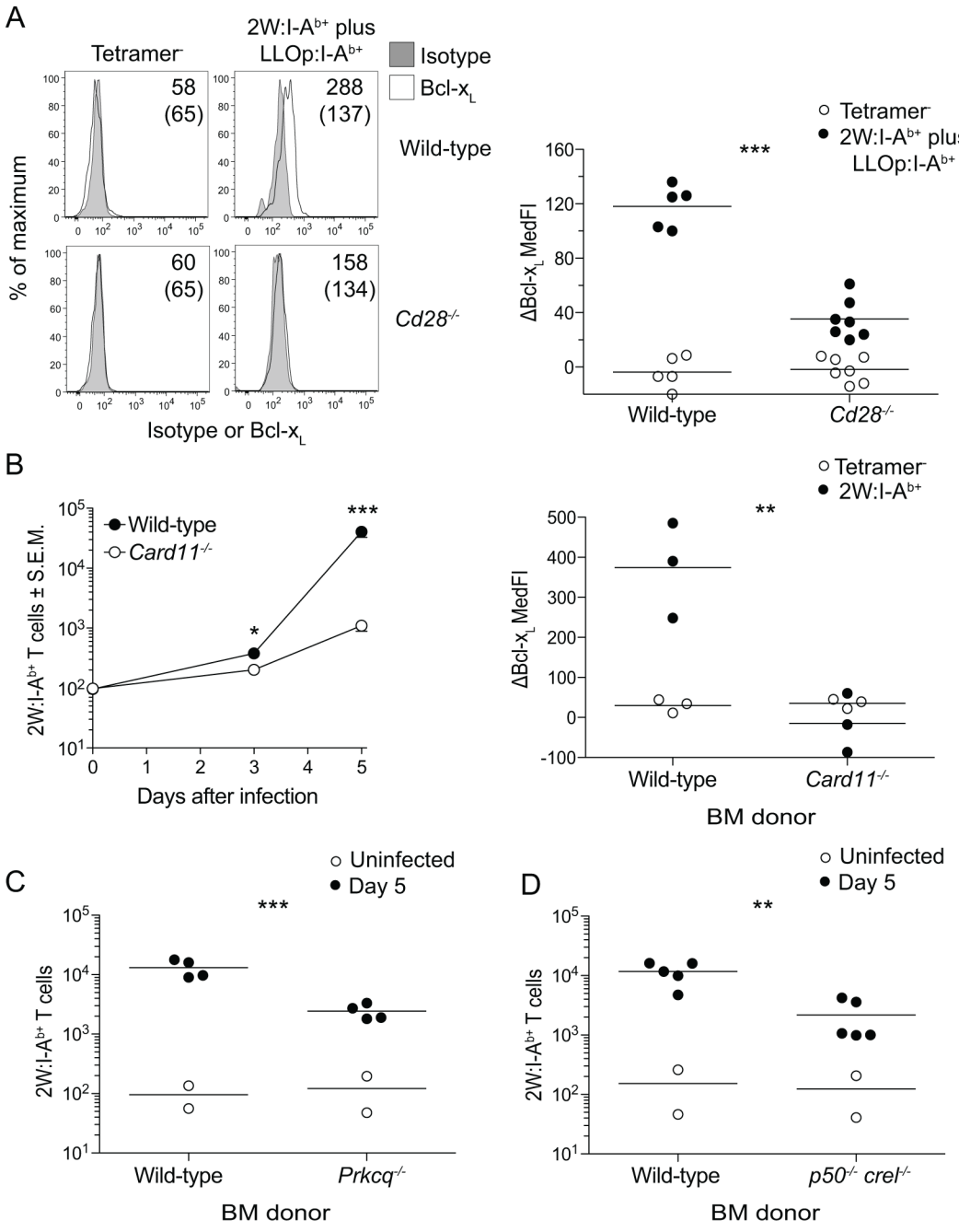

Figure 5. CD28 deficiency phenotypically resembles NFκB signaling deficiency *in vivo*.

(A) Histograms of isotype control or Bcl-x_L staining on tetramer$^-$ CD44^{low} or 2W:I-A^{b+} plus LLOp:I-A^{b+} wild-type or CD28-deficient mice 3 days after Lm-2W infection. Values for median fluorescence intensity of Bcl-x_L staining minus that of isotype control are shown on the right panel of (A). Mixed radiation chimeras made with wild-type and CARMA1-deficient (B), wild-type and PKCθ-deficient (C), or wild-type and p50/c-Rel-deficient (D) bone marrow cells. Mean numbers (n = 2 – 4) of wild-type or CARMA-deficient 2W:I-A^{b+} T cells in uninfected mice and mice at the indicated times after Lm-2W infection are shown on the left panel of (B). The right panel of (B) shows differences in median fluorescence intensity of Bcl-x_L staining minus that of isotype control for wild-type and CARMA1-

deficient cells. Horizontal lines indicate the mean values, and each symbol shows data from an individual mouse. A two-tailed Student's *t* test was used to compare the $\log_{10}$ values of tetramer$^+$ cells in Lm-2W infected groups, ** $p < 0.01$, *** $p < 0.001$.

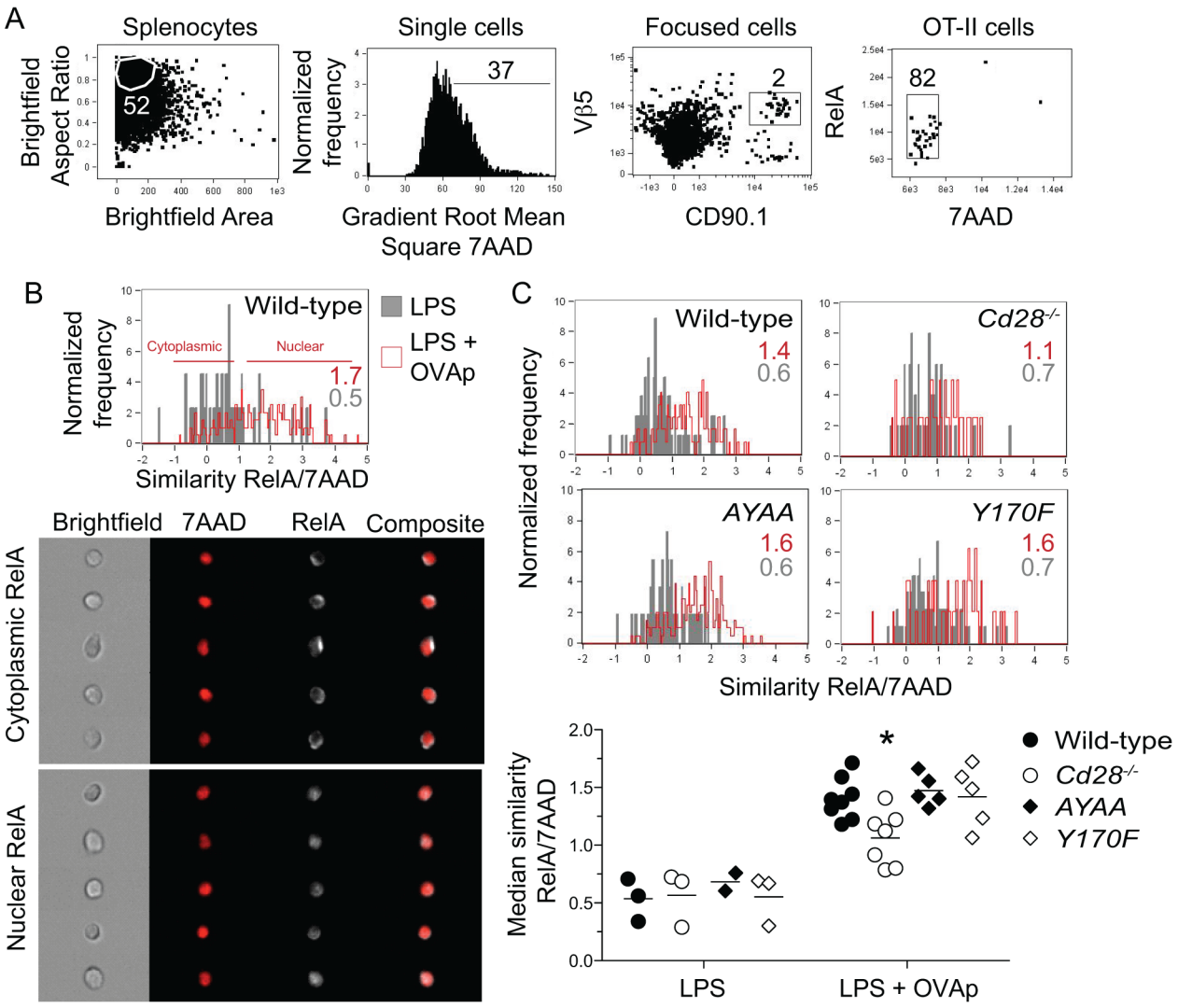

Figure 6. CD28 enhances p:MHCII-dependent nuclear translocation of RelA *in vivo* independently of the PYAP and YMNM motifs

Wild-type and CD28 mutant CD90.1$^+$ OT-II CD4$^+$ T cells were transferred intravenously into wild-type recipients. A day later, mice were injected intravenously with LPS. Two days after T cell transfer, some mice were injected intravenously with OVA peptide, and splenocytes were harvested 20 minutes later. (A) Flow cytometry plots show gating strategy used to measure RelA translocation in transferred OT-II cells within CD90.1-enriched samples. (B) Representative histograms of median RelA and 7AAD similarity in wild-type OT-II cells from LPS (gray) or LPS plus OVA peptide-injected mice (red) (top). Median RelA/7AAD similarity values are shown on each histogram for samples stimulated with LPS alone (gray) or LPS plus OVA peptide (red). Sample images of cytoplasmic and nuclear RelA staining in OT-II cells from the LPS plus OVA peptide sample are shown at the bottom. (C) Histograms of median RelA and 7AAD similarity in wild-type, CD28-deficient, *AYAA* and *Y170F* OT-II cells from LPS (gray) or LPS plus OVA peptide-injected mice (red). Median values for RelA and 7AAD similarity from individual mice (bottom). Horizontal lines on the graph on the bottom indicate mean values, and each symbol depicts a value from an individual mouse. Groups were compared by one-way ANOVA and

Bonferroni post-test, * $p < 0.05$. Graph shows pooled data from four independent experiments.